



April 29, 2009
NND-09-0065

U.S. Nuclear Regulatory Commission
Document Control Desk
Washington, DC 20555

ATTN: Document Control Desk

Subject: Virgil C. Summer Nuclear Station (VCSNS) Units 2 and 3 Combined License Application (COLA) - Docket Numbers 52-027 and 52-028 Supplement 2 Response to NRC Request for Additional Information (RAI) Letter No. 032

- Reference:
- 1) Letter from Ravindra G. Joshi (NRC) to Alfred M. Paglia (SCE&G), Request for Additional Information Letter No. 032 Related to SRP Section 2.5.4 for the Virgil C. Summer Nuclear Station Units 2 and 3 Combined License Application, dated February 12, 2009.
 - 2) Letter from Ronald B. Clary to (SCE&G) to the Document Control Desk, Response to NRC Request for Additional Information (RAI) Letter No. 032, dated March 16, 2009.
 - 3) Letter from Ronald B. Clary to (SCE&G) to the Document Control Desk, Supplement 1 to Response to NRC Request for Additional Information (RAI) Letter No. 032, dated March 27, 2009.

The enclosure to this letter provides the South Carolina Electric & Gas Company (SCE&G) response to the following RAI items included in the above referenced letter: 02.05.04-13, 20, 25, 29 and 30. The enclosure also identifies any associated changes that will be incorporated in a future revision of the VCSNS Units 2 and 3 COLA.

Should you have any questions, please contact Mr. Al Paglia by telephone at (803) 345-4191, or by email at apaglia@scana.com.

D083
NRO

I declare under penalty of perjury that the foregoing is true and correct.

Executed on this 29th day of April, 2009.

Sincerely,



Ronald B. Clary
General Manager
New Nuclear Deployment

AMM/RBC/am

Enclosure

c (with attachment):

Luis A. Reyes
Ravindra G. Joshi
Chandu Patel
John Zeiler
Stephen A. Byrne
Ronald B. Clary
Bill McCall
Kenneth J. Browne
Randolph R. Mahan
Kathryn M. Sutton
Amy M. Monroe
Courtney W. Smyth
John J. DeBlasio
Grayson Young
FileNet

NRC RAI Letter No. 032 Dated February 12, 2009

SRP Section: 2.5.4 – Stability of Subsurface Materials and Foundations

Question from Geosciences and Geotechnical Engineering Branch 1 (RGS1)

NRC RAI Number: 02.05.04-13

FSAR Section 2.5.4.2.2.1 indicates that the top of Layer V (sound rock) was based on estimates of RQD from the available boring samples as well as measured shear wave velocities determined from the suspension logger. Table 2.5.4-201 indicates that the top of Layer V can vary from as low as elevation 335' to as high as elevation 360'. Figure 2.5.4-211 indicates that measured RQD for sound rock varies from as low as 20% up to 100% with average RQD values exceeding 50%. Please provide information on the correlation of RQD with V_s as well as how average values were determined from the boring data for rock profiles that have such apparent non-uniformity with depth.

VCSNS RESPONSE:

Attached are 8 figures that show RQD and V_s values obtained from the 8 boreholes in which the P-S suspension logger was used (4 in Unit 2 and 4 in Unit 3). Note that all of the measured RQD and V_s values are included in these figures, not just those of sound rock.

As noted in FSAR Section 2.5.4.2.2.1, sound rock was generally assumed when RQD exceeded 50%, but RQD values in sound rock were, in fact, typically over 70%. FSAR Table 2.5.4-209, Summary of Engineering Properties, shows RQD for Unit 2 to be in the 80% to 100% range, and RQD for Unit 3 to be in the 90% to 100% range. These Table 2.5.4-209 values are well illustrated in the figures, with only a few RQD values falling below 80% in the Unit 2 borings and even less falling below 90% in the Unit 3 borings. Very few rock cores were obtained in the MWR (RQD values less than 50%).

As would be expected, there is general correlation between RQD and V_s . In the Unit 2 borings, when RQD drops below about 80%, there is a noticeable reduction in V_s (except in B-207 around El. 330 ft, where no reduction in V_s was recorded). Similarly in the Unit 3 borings, when RQD drops below about 90%, there is a noticeable reduction in V_s .

Since there is no dip or bedding in the sound rock, the average values are based on 5 ft intervals of elevation. Note that in FSAR Figure 2.5.4-211(a), which includes values from 15 borings in Unit 2, there are a few RQD values less than 50%. In these cases, there was nothing in the core description to indicate partial or moderate weathering (PWR or MWR) and so the cores were counted as sound rock.

This response is PLANT SPECIFIC.

ASSOCIATED VCSNS COLA REVISIONS:

No COLA changes have been identified as a result of this response.

ASSOCIATED ATTACHMENTS:

Figures 02.05.04-13.1 through 02.05.04-13.8

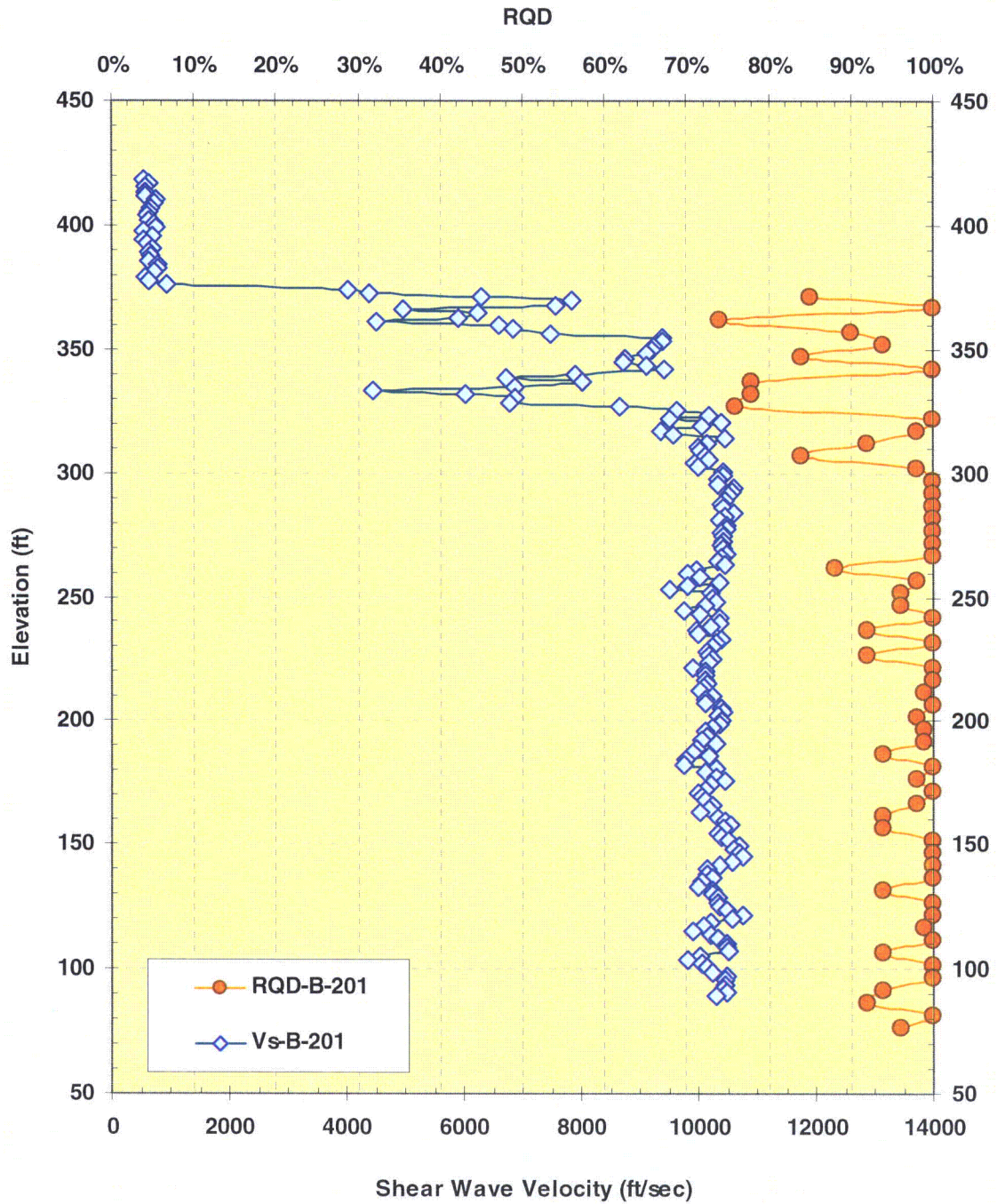


Figure 02.05.04-13.1: Boring B-201 - RQD and V_s versus Elevation

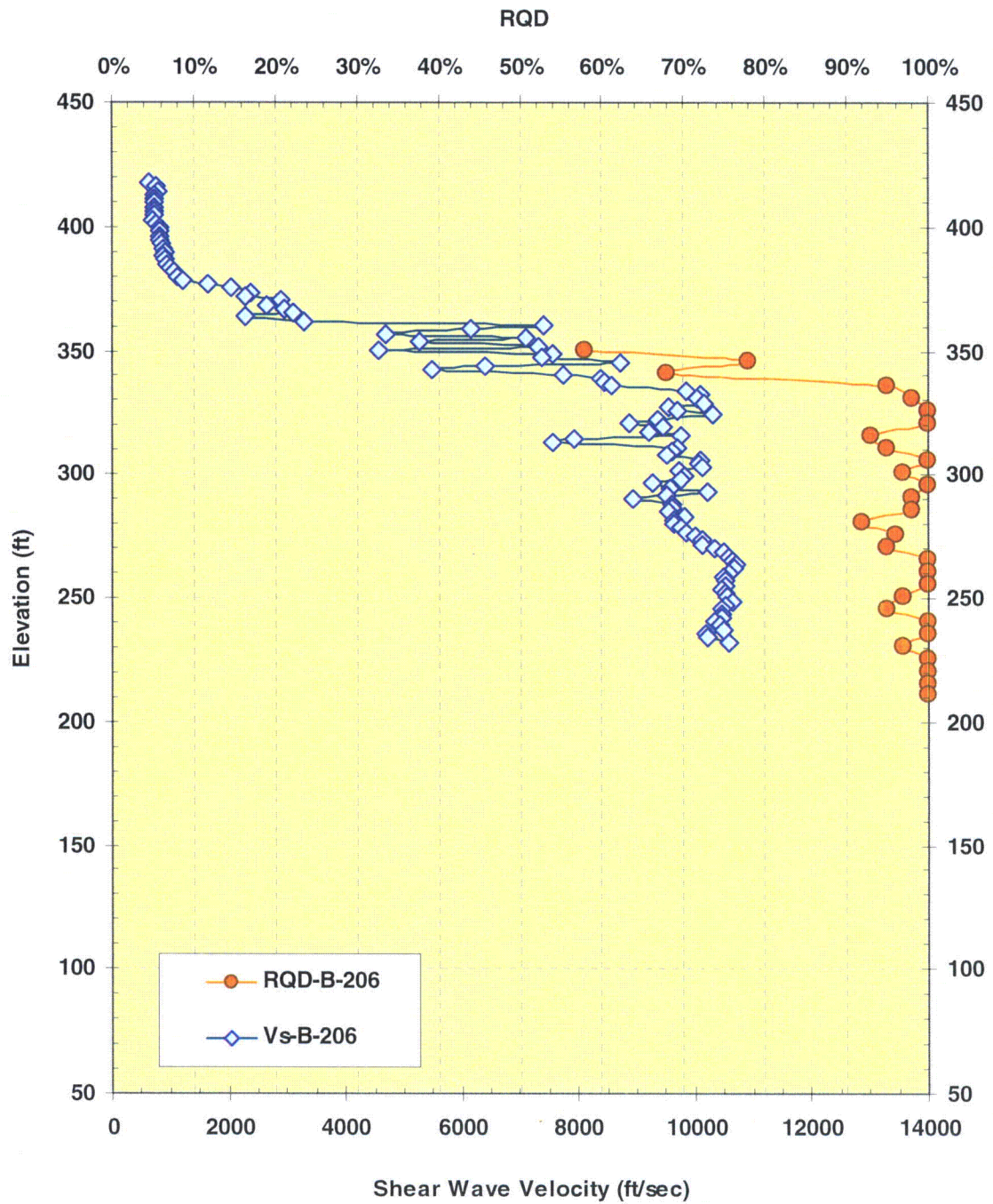


Figure 02.05.04-13.2: Boring B-206 - RQD and V_s versus Elevation

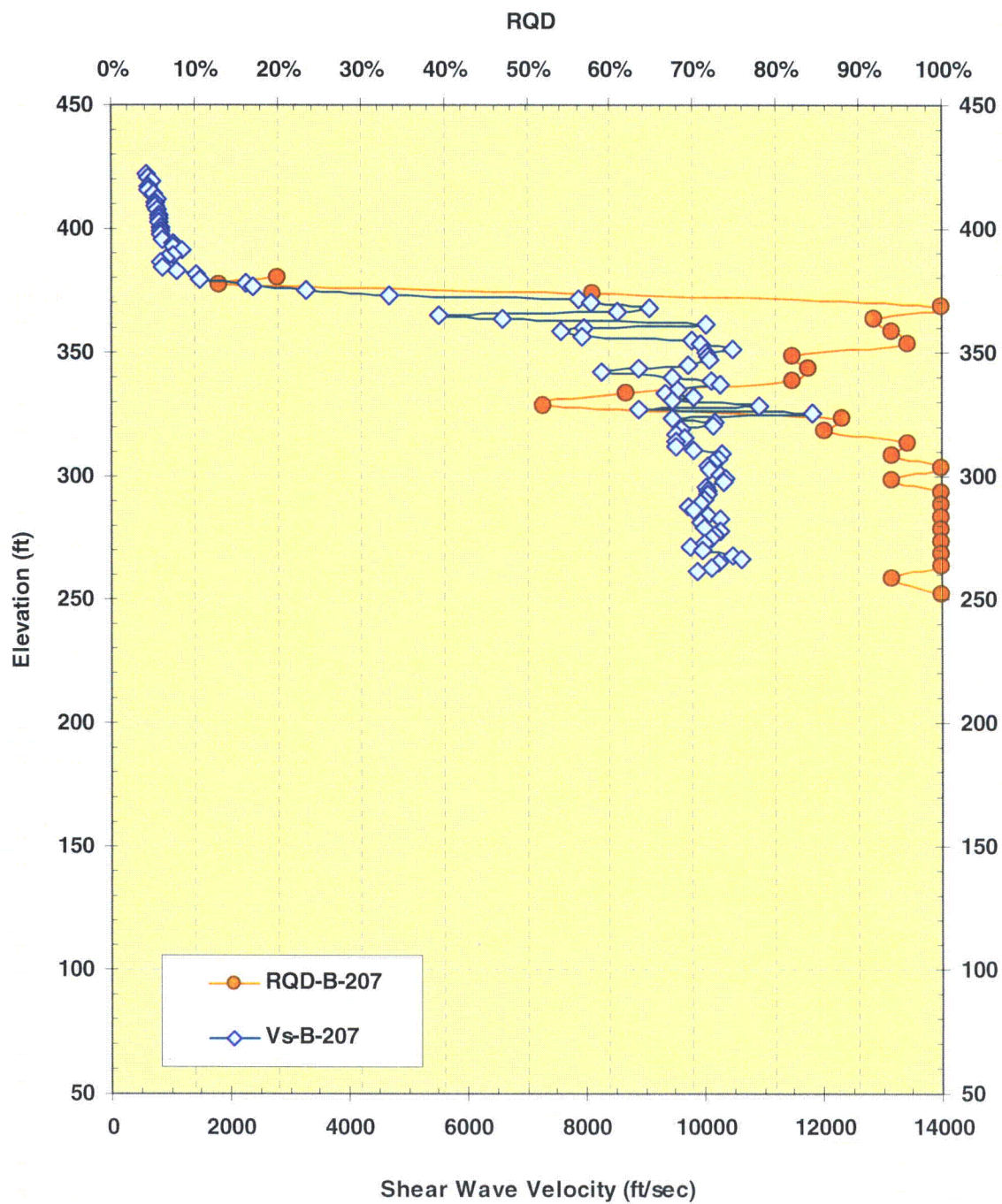


Figure 02.05.04-13.3: Boring B-207 - RQD and V_s versus Elevation

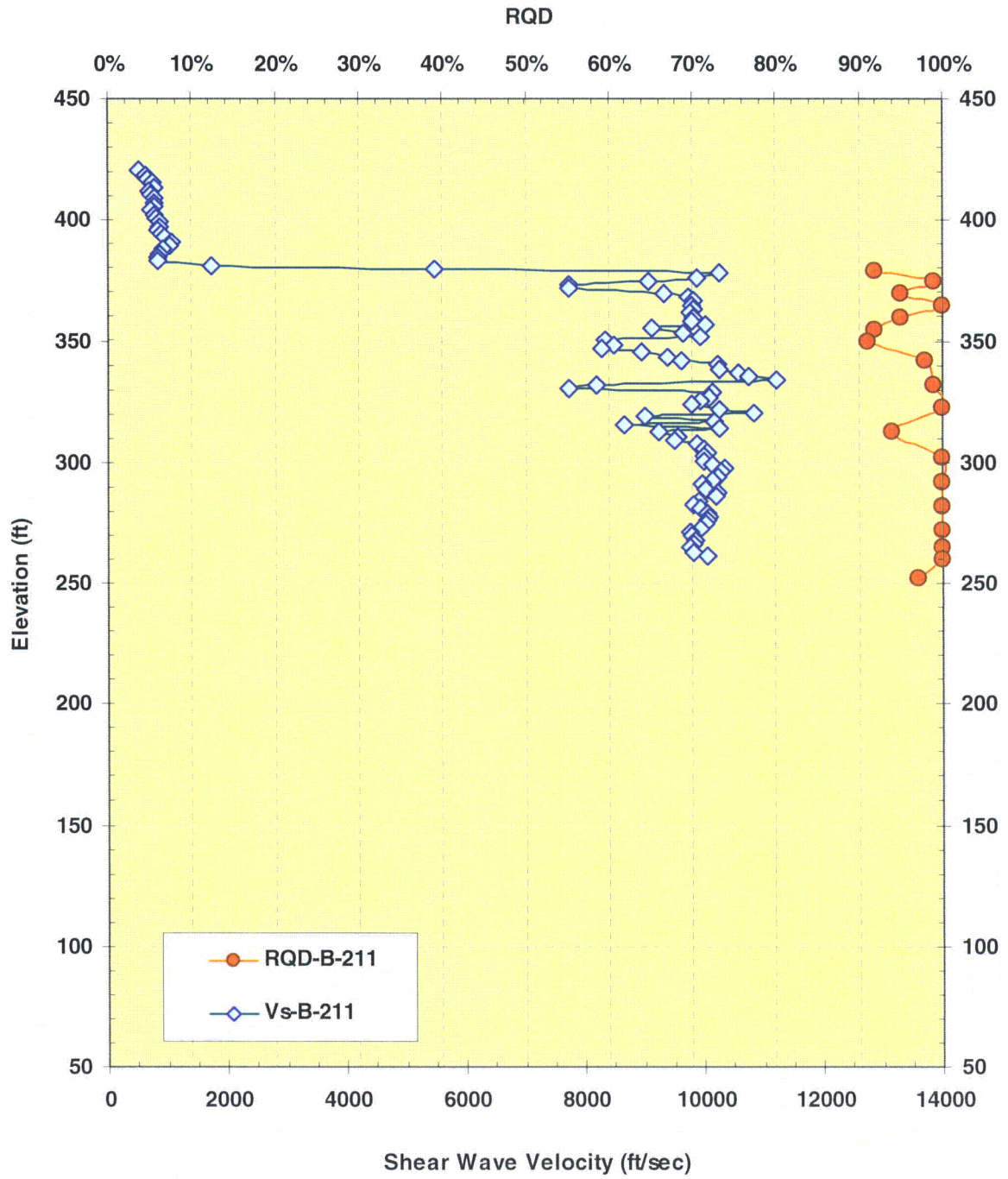


Figure 02.05.04-13.4: Boring B-211 - RQD and V_s versus Elevation

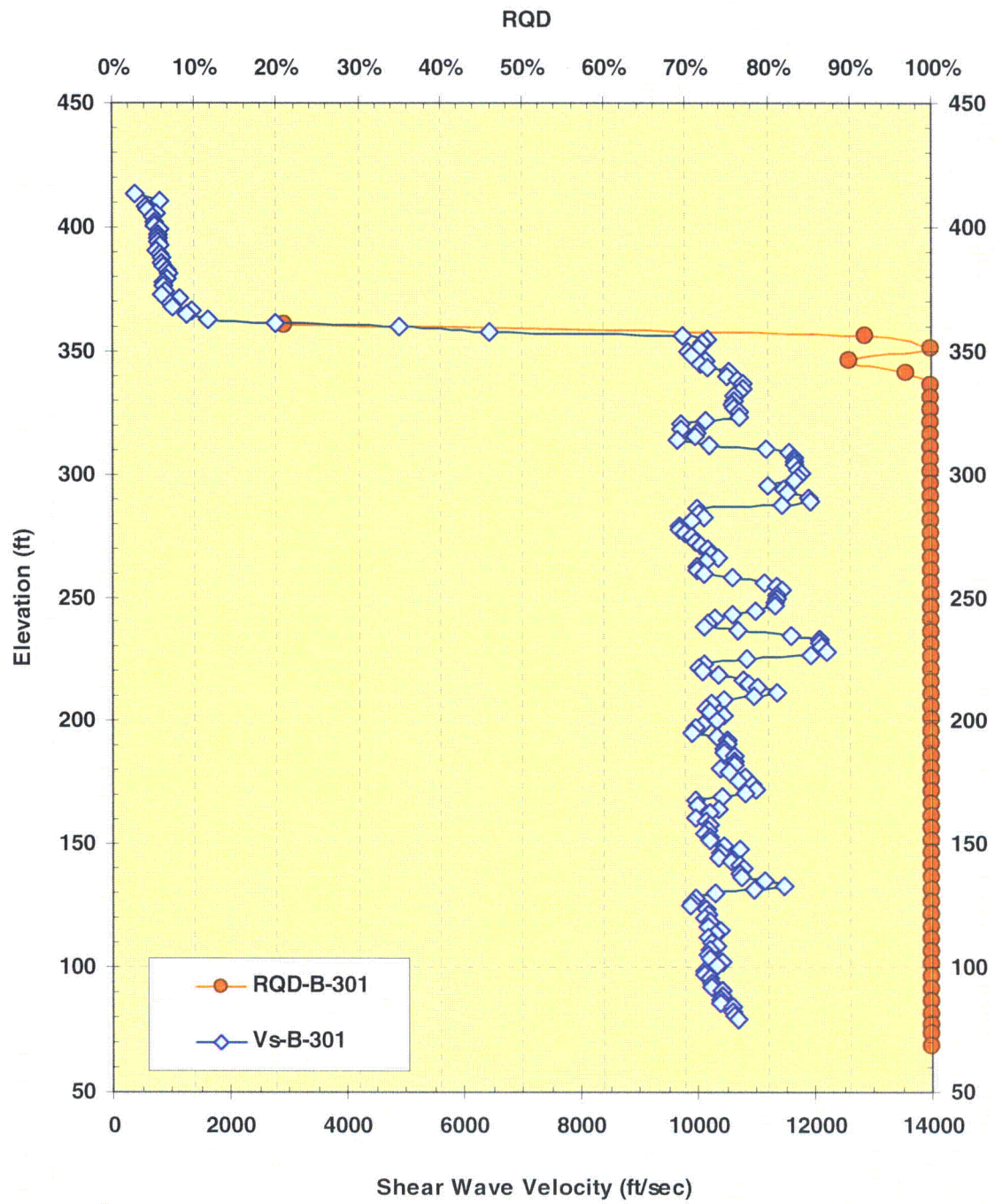


Figure 02.05.04-13.5: Boring B-301 - RQD and V_s versus Elevation

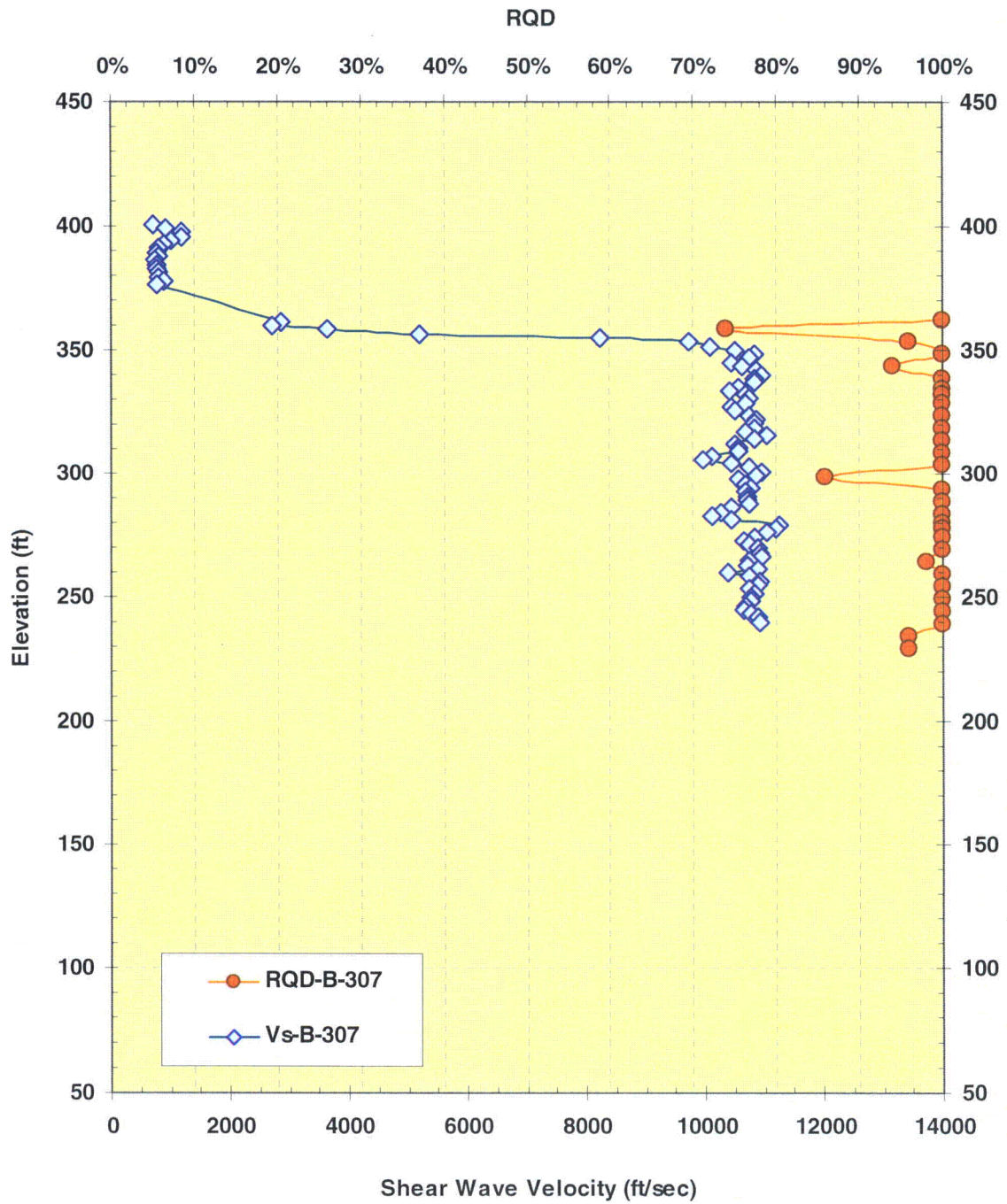


Figure 02.05.04-13.7: Boring B-307 - RQD and V_s versus Elevation

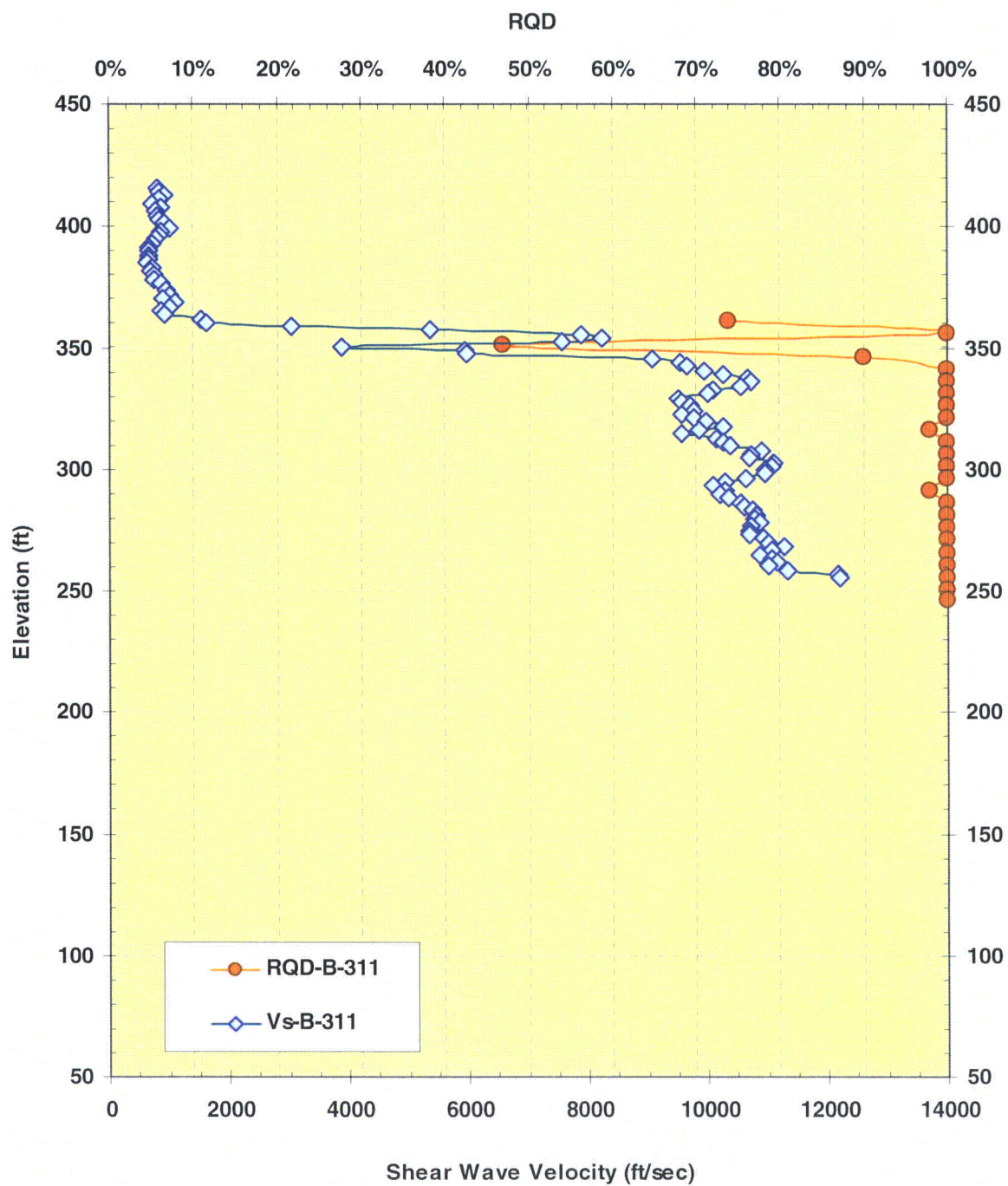


Figure 02.05.04-13.8: Boring B-311 - RQD and V_s versus Elevation

NRC RAI Letter No. 032 Dated February 12, 2009

SRP Section: 2.5.4 – Stability of Subsurface Materials and Foundations

Question from Geosciences and Geotechnical Engineering Branch 1 (RGS1)

NRC RAI Number: 02.05.04-20

FSAR Section 2.5.4.4.2 describes the process of installing the steel or PVC casing in the eight holes used for the suspension logger measurements. The description indicates that the casings were removed from the hole and “in some cases, acceptable results were obtained from the suspension P-S logger, provided the casing was well grouted into the soil.” Please provide information to indicate how these results were judged to be adequate, how the grouting was evaluated to indicate a well-grouted condition, and if the removal of the casing caused disturbance of the surrounding soil. Also in this description, please include the impact of this procedure on measurements through the PWR and MWR materials.

VCSNS RESPONSE:

Attachment E of the MACTEC Geotechnical Data Report, “Geophysical Test Results” (see COLA Part 11) lists the 5 criteria on which the data quality of the P-S suspension logging velocity measurements are judged:

1. Consistent data between receiver to receiver (R1 – R2) and source to receiver (S – R1) data
2. Consistent relationship between P-wave and S_H-wave (excluding transition to saturated soils)
3. Consistency between data from adjacent depth intervals
4. Clarity of P-wave and S_H-wave onset, as well as damping of later oscillations
5. Consistency of profile between adjacent borings, if available

Attachment E indicates the suspension logger tests that were conducted in cased borings in the soil (PVC casing), and the tests that were conducted in uncased borings. It provides an assessment of the quality of the soil velocity data based on the above criteria. Although the casing was removed from each boring before the hole was abandoned, the uncased holes used for velocity measurements were actually separate holes drilled 10 ft away from the original holes, i.e., the velocity data were not measured in the holes after casing had been removed.

The quality of the velocity data in the soil are tabulated as follows.

Boring	Cased/Uncased	Quality of Velocity Data in Soil
B-201	Cased	Fair
B-206	Cased	Poor due to poor coupling of PVC casing
B-207	Cased	Fair
B-211	Cased	Poor – not used
B-211A	Uncased	Excellent
B-301	Cased	Good
B-306	Cased	Data not interpretable - not used
B-307	Cased- from 26 to 41 ft depth.	Fair
B-307	Uncased to 26 ft depth	Fair
B-311	Cased	Good

FSAR Figures 2.5.4-228 and 2.5.4-229 show the shear wave velocities in the soil to be very consistent (and in good agreement with the shear wave velocities obtained from the CPTs). FSAR Figures 2.5.4-231 and 2.5.4-232 show similarly consistent compression wave velocities (no CPT data).

Soil sampling was stopped in the borings when SPT refusal was reached. This typically occurred at the top of the PWR. Rock coring created an uncased hole beneath this point of refusal, and thus most of the PWR and all of the MWR measurements were taken in uncased holes, and so were not affected by the quality of the coupling between the PVC casing and the soil.

This response is PLANT SPECIFIC.

ASSOCIATED VCSNS COLA REVISIONS:

FSAR Section 2.5.4.4.2, first part of second paragraph will be revised in a future revision of the COLA as follows:

“For most of the tests, the eight borings were logged as partially-cased borings, filled with clear water or polymer-based drilling mud, with a 4-inch PVC or steel casing placed in the top 40 to 60 feet of softer soil above bedrock contact during the measurements of the lower rock portions of the borings. ~~The casing was then removed and measurements were performed in the upper soil portion of the borings.~~ (In some cases, acceptable results were obtained from the suspension P-S logger in the PVC-cased soil hole, provided the casing was well grouted into the soil.) Where lack of coupling occurred between the casing and the soil leading to poor quality velocity measurements, a separate uncased hole was drilled in the soil about 10 feet from the original hole, and P-S suspension velocity readings were taken in the uncased hole.”

Enclosure 1
Page 13 of 34
NND-09-0065

ASSOCIATED ATTACHMENTS:

None

NRC RAI Letter No. 032 Dated February 12, 2009

SRP Section: 2.5.4 – Stability of Subsurface Materials and Foundations

Question from Geosciences and Geotechnical Engineering Branch 1 (RGS1)

NRC RAI Number: 02.05.04-25

FSAR Section 2.5.4.7.1.2 describes the process used to estimate the velocity profile through the structural backfill. Figure 2.5.4-238 indicates that the best estimate surface velocity will be about 800 fps. This value seems high as compared to results determined at other sites. Please provide the basis for this estimate, how the results will be determined after fill placement, and please describe the impact on the evaluation if the actual surface velocity is found to be significantly lower.

VCSNS RESPONSE:

The basic equations used to compute the shear wave velocity of the fill were:

$$G_{\max} = 240 \cdot N^{0.8} \text{ (ksf)} \quad \text{(NAVFAC 1982)}$$

where G_{\max} = low strain shear modulus
 N = SPT N-value

$$G_{\max} = K_2 \cdot (\sigma'_m)^{0.5} \text{ (psf)} \quad \text{(Seed & Idriss 1970)}$$

where, σ'_m = mean principal effective stress (psf)
 K_2 = a parameter reflecting primarily the effect of void ratio or relative density and the strain amplitude of the motions.

As noted in FSAR Section 2.5.4.7.1.2, the computed shear wave velocity values were adjusted for surcharge loading from locked-in stresses from compaction. Because of the inherent uncertainty involved with estimating shear wave velocity profiles, FSAR Figure 2.5.4-238 also shows the shear wave velocity values for Mean +/- 1 Standard Deviation.

The computed shear wave velocity values for the structural fill were also compared to the measured values for the saprolite which will be replaced by the fill. These values are tabulated as follows:

Depth, Ft	Shear Wave Velocity, Ft/Sec			
	Structural Fill		Avg. Measured Saprolite Values.	
	Mean – 1 Std Dev	Mean	Unit 2	Unit 3
0-5	628	811	582	827
5-10	672	867	649	688
10-15	708	913	716	826
15-20	739	954	751	815
20-25	767	990	830	889
25-30	792	1022	826	819
30-35	815	1051	913	790
35-40	813	1049	842	834
40-45	825	1064	995	872
45-50	835	1077	1017	926

The saprolites have an average SPT N-value of 20 blows/ft compared with 30 blows/ft for the structural fill, and are generally silty fine sands, with some mica, compared to the much cleaner, coarser, and better graded structural fill. It would be expected that the structural fill would have a significantly higher shear wave velocity profile than the saprolite. The mean structural fill values are higher than the measured saprolite values. However, the lower bound fill values (assumed as a standard deviation below the mean) fall between the saprolite values in the top 10 ft and are lower than the saprolite values below 10 ft.

FSAR Figure 2.5.4-228 indicates excellent agreement between the shear wave velocities measured in the saprolite using the P-S Suspension Logger and the seismic CPT. Thus, if shear wave velocity measurements are made in the structural fill, then both types of measuring equipment are expected to produce similar results.

Structural fill will not be placed under the seismic Category I nuclear island, and, as indicated in AP1000 DCD Section 3.7.2.1.2, the evaluation of the seismic response of the AP1000 neglected any effects of the fill surrounding the nuclear island. Thus, measured values of shear wave velocity for the seismic Category I structures are immaterial. The FIRS for the non-seismic Category I annex building was computed using a randomized shear wave velocity profile through the structural fill, i.e., variations in the shear wave velocity were accounted for. If the shear wave velocity of the compacted fill is measured (bearing in mind that it is not a seismic Category I structure), and the values beneath the foundation are significantly below the estimated values, then a new FIRS will be developed and compared with the CDRS of the structure. However, note that the foundation of the annex building is 5 ft below final grade. If the shear wave velocity of the structural fill is measured, and (1) measurements are taken from final grade with the annex building already constructed, and (2) these

measurements are taken immediately adjacent to the foundation so that the confining pressures due to the considerable structure loading are at least partly taken into account, then the measured shear wave velocity at foundation level will almost certainly be as much as the mean estimated value (tabulated above) at that depth.

References:

NAVFAC (1982). Naval Facilities Engineering Command. "Foundations & Earth Structures", *Design Manual 7.02*, Alexandria, VA.

Seed, H.B., and Idriss, I.M. (1970). "Soil Moduli and Damping Factors for Dynamic Response Analyses" Report No. EERC 70-10, University of California, Berkeley, December.

This response is PLANT SPECIFIC.

ASSOCIATED VCSNS COLA REVISIONS:

No COLA changes have been identified as a result of this response.

ASSOCIATED ATTACHMENTS:

None

NRC RAI Letter No. 032 Dated February 12, 2009

SRP Section: 2.5.4 – Stability of Subsurface Materials and Foundations

Question from Geosciences and Geotechnical Engineering Branch 1 (RGS1)

NRC RAI Number: 02.05.04-29

FSAR Section 2.5.4.10.3 indicates that active and at-rest pressures are used for the evaluation of lateral wall pressures. The design of the AP1000 is based on considerations of the development of passive pressures due to horizontal seismic loadings, and how the total lateral load is distributed to both lateral wall loads and base shear. The pressure diagrams shown in FSAR Figures 2.5.4-243 and 244 indicate dynamic pressures distributions, which do not follow the anticipated results typically calculated from the recommendations in ASCE 4-98 and 43-05. Please provide information justifying the calculation of these pressure diagrams and how they compare to the estimates used in the AP1000 design process.

VCSNS RESPONSE:

Active condition

FSAR Figure 02.05.04-243 – active lateral earth pressure – was developed using the Mononobe-Okabe method to calculate dynamic active lateral earth pressures. This figure applies to the prospective yielding retaining walls at the site, rather than the earth-retaining walls of the nuclear island structures. As ASCE 4-98, Section 3.5.3.3 states, the Mononobe-Okabe approach may be used to establish dynamic soil pressures, provided that wall displacements required to develop the active earth pressure can be tolerated without loss of wall function. According to Reference 1, p. 1773, use of the horizontal ground acceleration ($k_h \cdot g$) for design at the level of the base of the wall may result in underestimating the movements; it is preferable to use the acceleration (and the velocity) at the surface of the backfill, or to use an average of the values between the surface and the base of the wall. The maximum peak horizontal ground acceleration of 0.55g (obtained for Unit 2 in-situ soils as shown in RAI Figure 02.05.04-29.1) was conservatively used for developing the seismic active earth pressure diagrams (i.e., $k_h=0.55$), even though the peak horizontal ground acceleration obtained for the structural fill was 0.38g (from RAI Figure 02.05.04-29.6 at 100 Hz).

The active lateral earth pressure is shown in RAI Figure 02.05.04-29.2, which includes a surcharge pressure of 500 psf x 0.26 ($K_A=0.26$), and a wall height of 40 ft (the standard value in AP 1000 design).

At-rest condition

Due to the limitation of the Mononobe-Okabe based methods for embedded walls of structures such as the nuclear island, Reference 2 recommends a method for

computing the dynamic component of seismic at-rest lateral earth pressure. FSAR Figure 2.5.4-244 – at-rest lateral earth pressure – was developed using this (Ostadan) method. This figure applies to the embedded walls of the nuclear island structures. Since the base of the wall is founded on sound rock, the horizontal ground acceleration ($k_h \cdot g$) for design was obtained from the horizontal Ground Motion Response Spectrum (GMRS) on hard rock shown in FSAR Figure 2.5.2-246.

Supplementary At-Rest Analyses using ASCE 4-98 Method

Following ASCE 4-98 (Reference 3), Section 3.5.3.2, the dynamic component of seismic at-rest lateral earth pressure is redeveloped for the earth-retaining walls of the nuclear island structures. This elastic solution displayed in a nomograph is shown in RAI Figure 02.05.04-29.3. In this figure, a dimensionless normal stress at 1.0g horizontal earthquake acceleration is developed for a normalized depth at a given Poisson's ratio.

The lateral dynamic soil pressure is then recalculated for various depth intervals using the site specific horizontal earthquake acceleration by rearranging the dimensionless normal stress equation and multiplying by the site-specific acceleration. Using the following parameters, the at-rest lateral earth pressure distribution including the dynamic component is recalculated and illustrated in RAI Figure 02.05.04-29.4. Note that this figure also illustrates the compaction-induced lateral earth pressures caused by heavy compactors for at-rest earth pressure conditions (refer to the response to RAI 2.5.4-30 for detailed information on calculation of compaction-induced lateral earth pressures) and a vertical surcharge of 2,500 psf. Note that the vertical areal surcharge of 2,500 psf equates to a lateral surcharge pressure of 1,250 psf ($K_0=0.5$), which exceeds the AP 1000 maximum lateral static plus dynamic design surcharge pressures.

Wall height = 40 ft
Total unit weight = 125 pcf
Poisson's ratio = 0.35
Horizontal ground acceleration = 0.38g

The site-specific horizontal acceleration is calculated using the ground surface acceleration response spectrum (ARS) at 5% damping. The ARS at ground surface for low and high frequency events for 10^{-4} and 10^{-5} probabilities, presented in RAI Figure 02.05.04-29.5, was previously obtained for Unit 2 structural fill (Annex Building). By applying the following calculation steps to the ARS data, the peak ground acceleration is calculated and presented in RAI Figure 02.05.04-29.6 as a function of frequency. The horizontal ground acceleration (0.38g) used in the ASCE 4-98 method is chosen from RAI Figure 02.05.04-29.6 at 100 Hz.

- 1) Take the maximum of (HF4, LF4) gives 10^{-4} PGA
- 2) Take the maximum of (HF5, LF5) gives 10^{-5} PGA
- 3) $AR(PGA) = [10^{-5} \text{ PGA}] / [10^{-4} \text{ PGA}]$
- 4) $DF = 0.6 \times AR^{0.80}$
- 5) $FIRS(PGA) = \max[[10^{-4} \text{ PGA}] \times \max(1, DF), 0.45 \times [10^{-5} \text{ PGA}]]$

where, HF4 is high frequency event with 10^{-4} probability
LF4 is low frequency event with 10^{-4} probability
HF5 is high frequency event with 10^{-5} probability
LF5 is low frequency event with 10^{-5} probability
AR is the ground motion slope ratio of spectral accelerations
DF is a design factor
FIRS is the Foundation Input Response Spectrum

For comparison purposes, the load combinations used in the AP 1000 below-grade wall design are provided. AP 1000 maximum design pressures in E-W and N-S directions from Westinghouse Electric Company (WEC), and the site specific total at-rest lateral earth pressures from RAI Figure 02.05.04-29.4 are plotted in Figure 02.05.04-29.7. Comparison of these pressure diagrams indicates that AP 1000 maximum design pressures envelope the site-specific total at-rest lateral earth pressures.

References

1. Whitman, R.V. (1991) "Seismic Design of Earth Retaining Structures," *Proc. 2nd International Conference on Recent Advances in Geotechnical Earthquake Engineering and Soil Dynamics*, St. Louis, MO, pp. 1767-1778.
2. Ostadan, F. and White, W.H. (1998) "Lateral Seismic Soil Pressure, An Updated Approach," *US-Japan SSI Workshop*, United States Geological Survey, Menlo Park, California, September 22-23.
3. ASCE 4-98. (2000) *Seismic Analysis of Safety-Related Nuclear Structures and Commentary*. ASCE, Reston, VA.

This response is PLANT SPECIFIC.

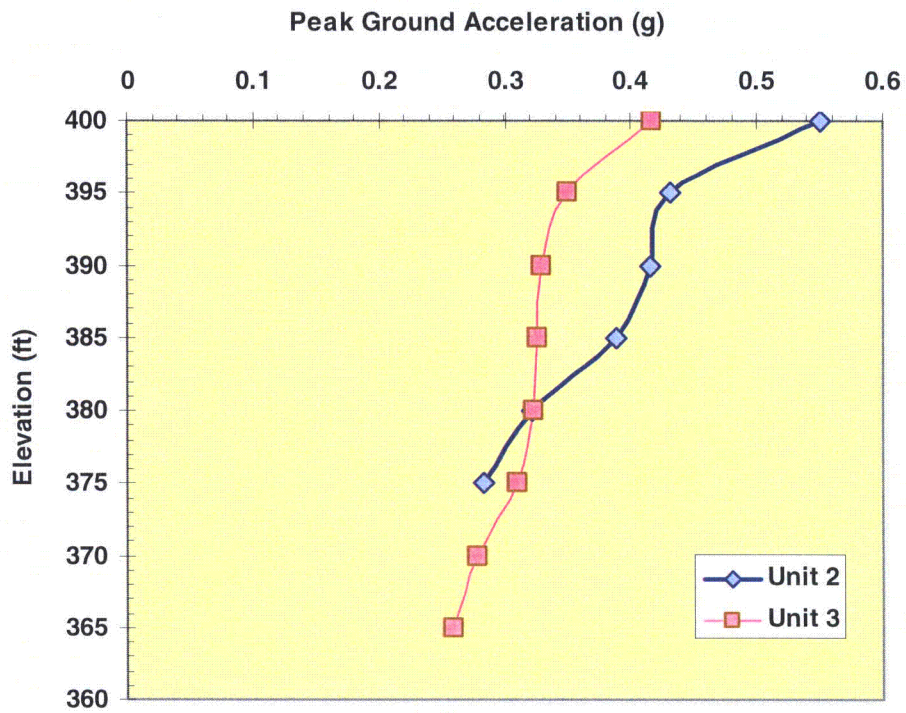
ASSOCIATED VCSNS COLA REVISIONS:

1. The fifth sentence of the first paragraph of FSAR Subsection 2.5.4.10.3 will be revised as follows:

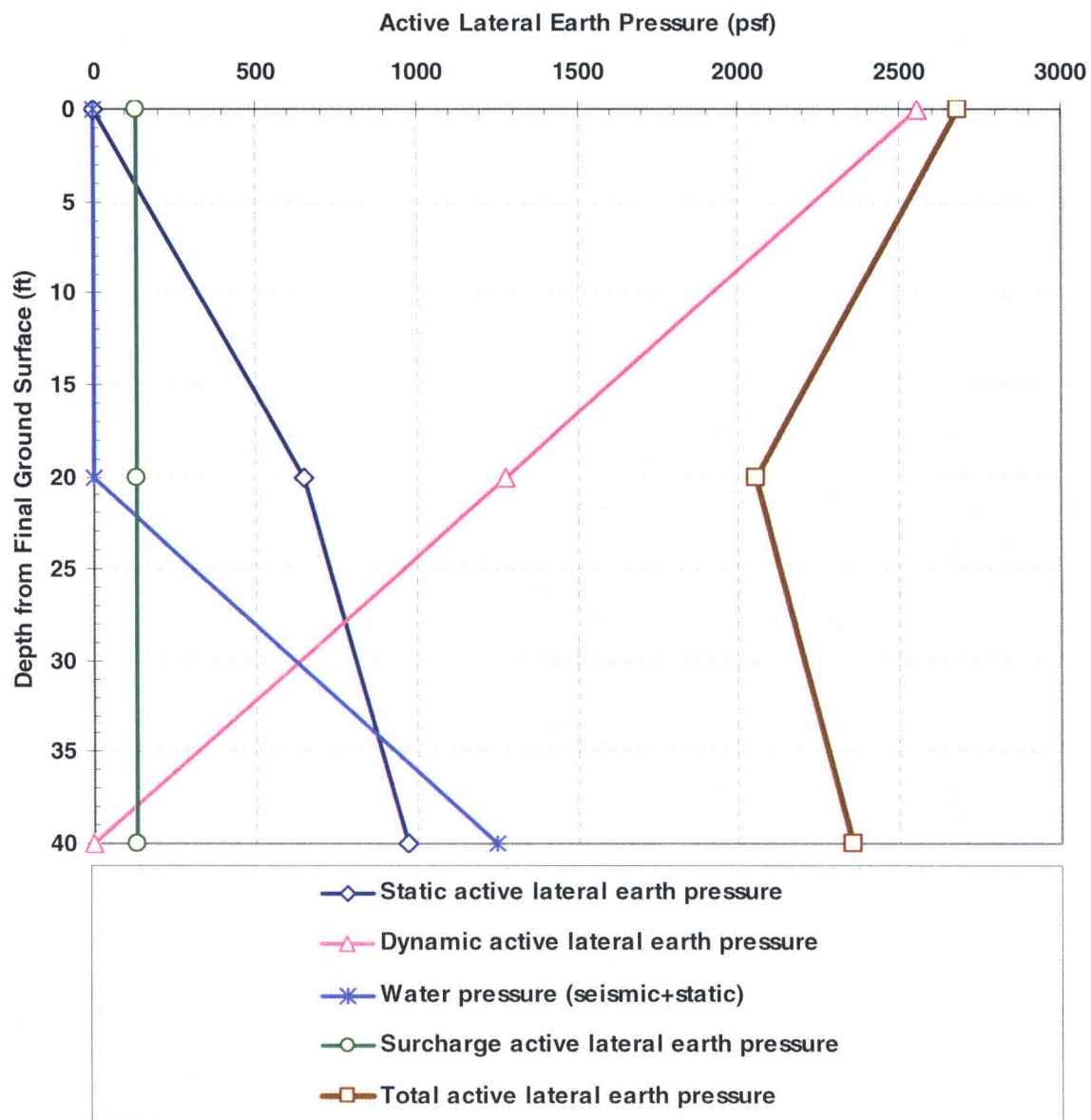
A conservative surcharge pressure of 500 psft was used. The area-wide surcharge pressures of 500 psf and 2,500 psf were conservatively used under active and at-rest conditions, respectively.

ASSOCIATED ATTACHMENTS:

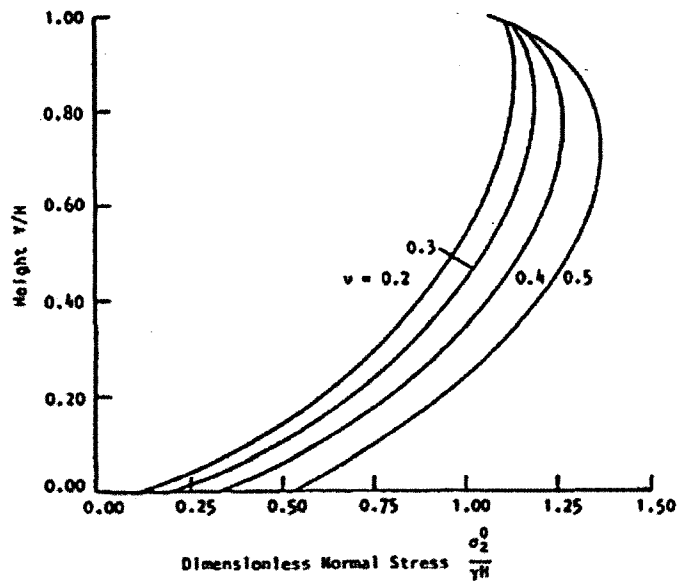
RAI Figures 02.05.04-29.1 through 02.05.04-29.7



RAI Figure 02.05.04-29.1: Peak ground acceleration (from FSAR 2.5.4-242)



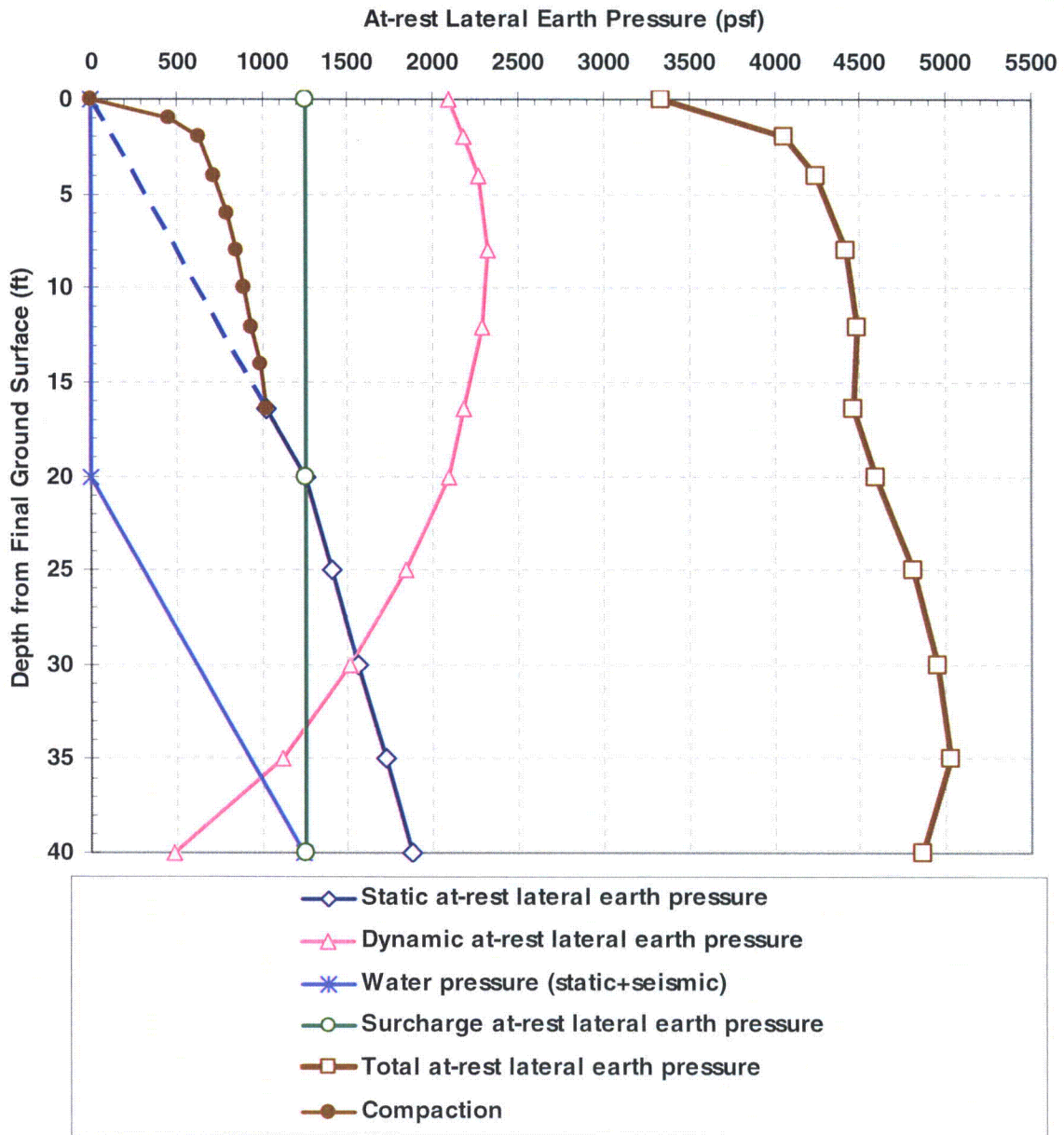
RAI Figure 02.05.04-29.2: Active lateral earth pressure



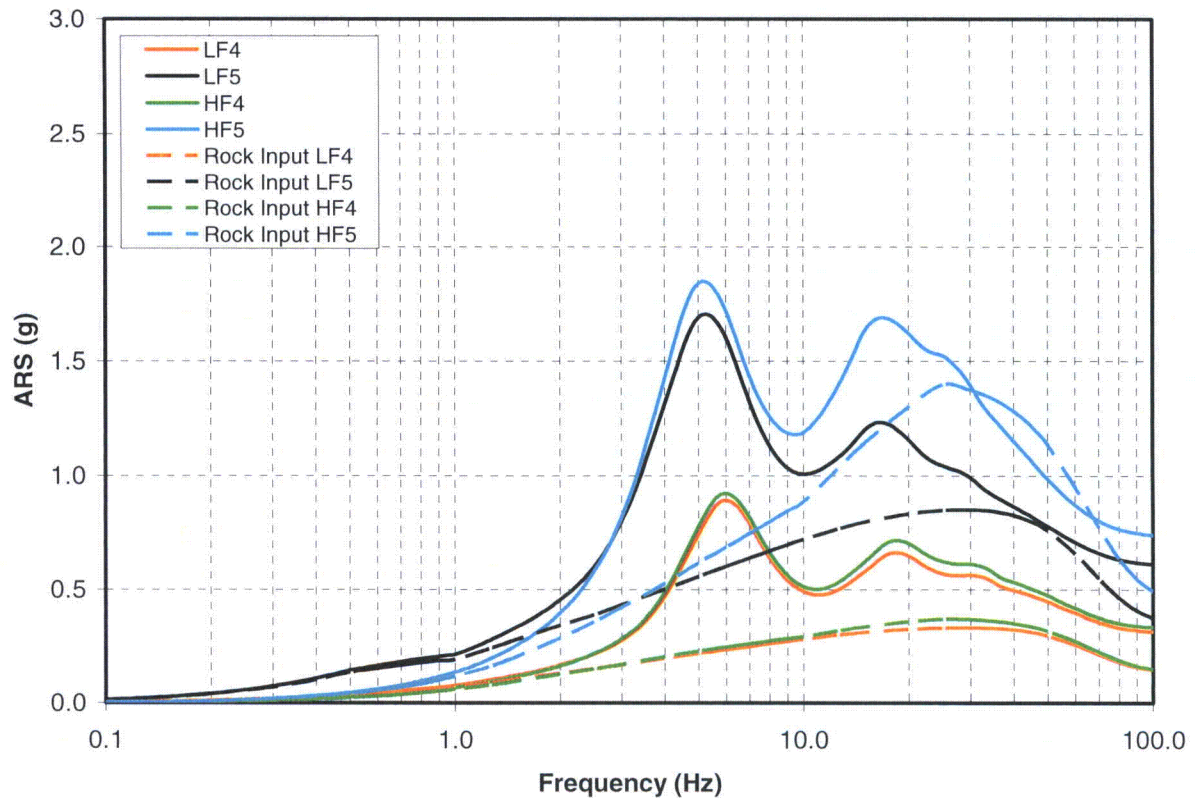
Explanation

- H = embedment height
- y = distance from base of retaining structure
- γ = soil unit weight
- ν = Poisson's ratio
- σ_2^0 = lateral dynamic soil pressure against the retaining structure for 1.0g horizontal earthquake acceleration

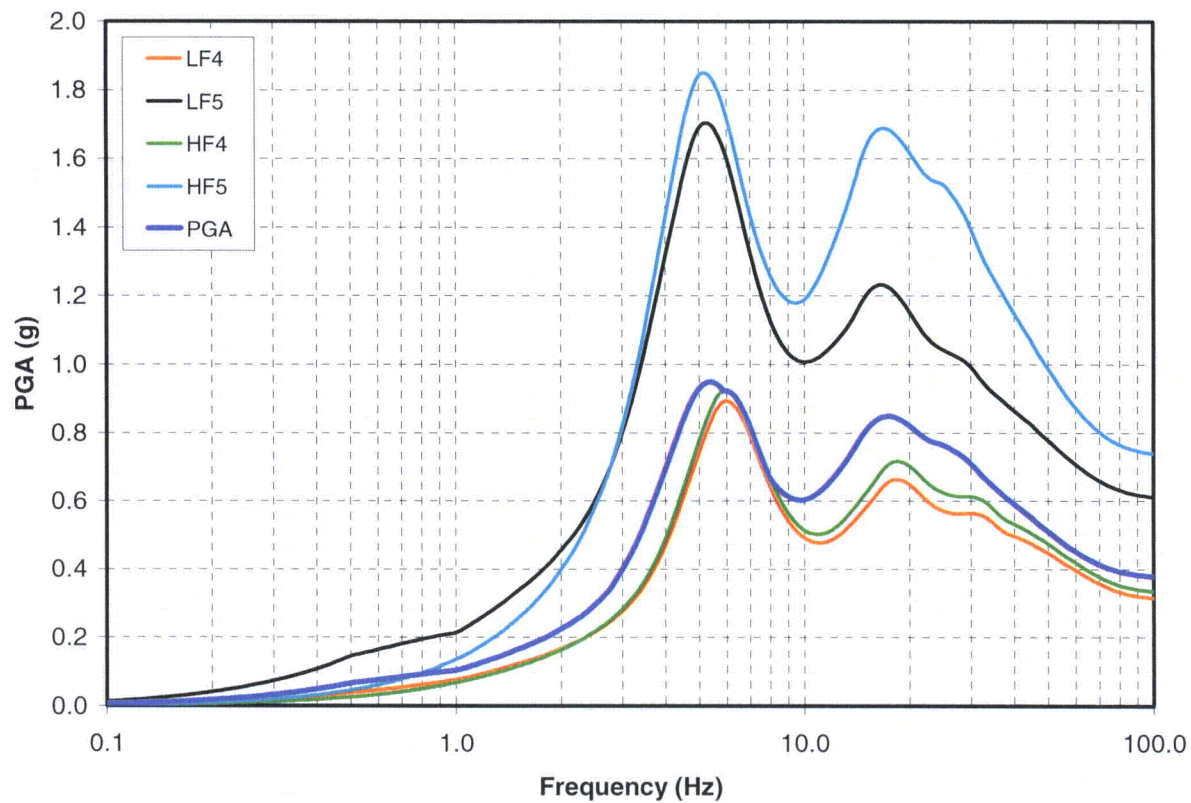
RAI Figure 02.05.04-29.3: Elastic solution (from ASCE 4-98, p. 36)



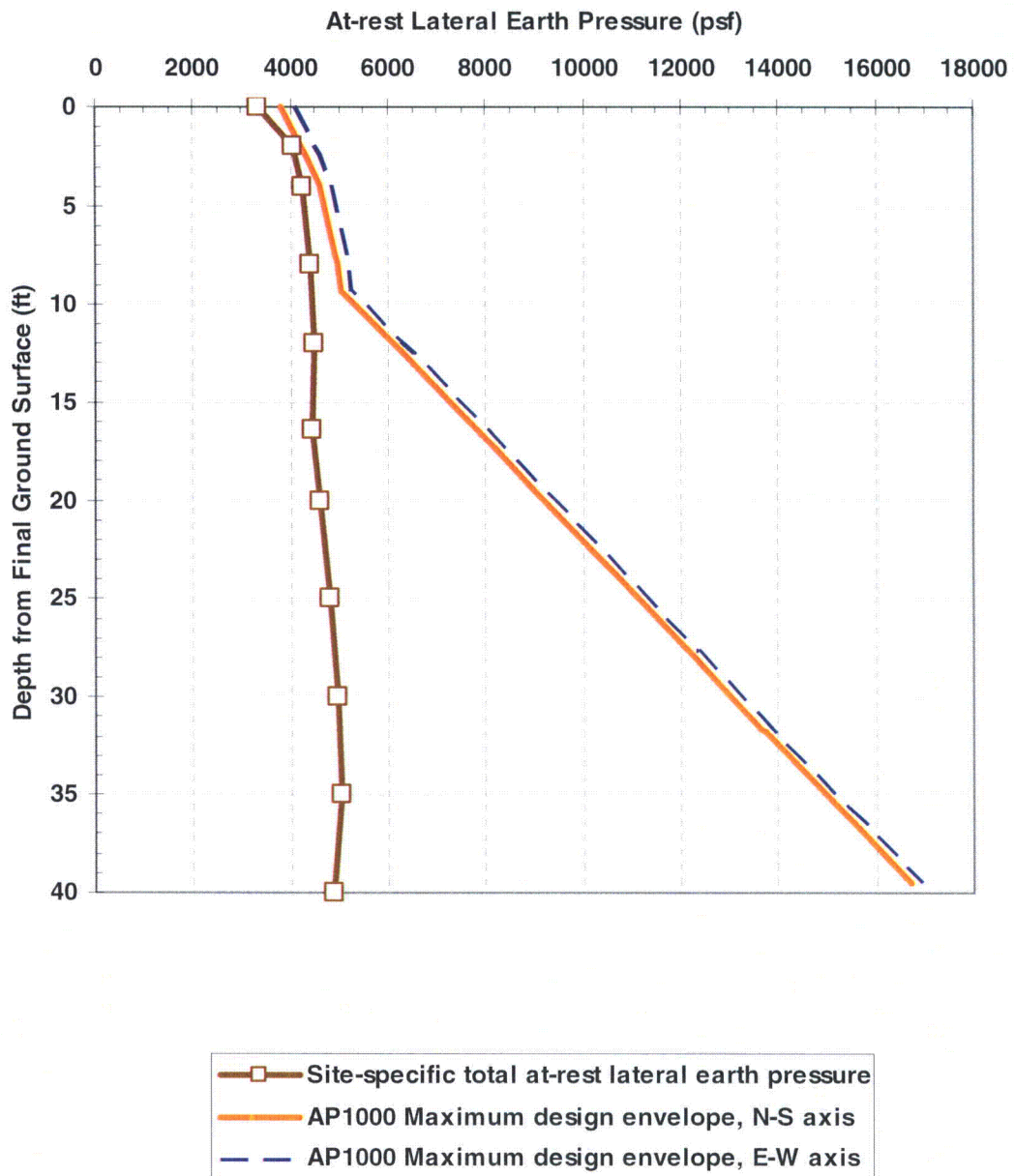
RAI Figure 02.05.04-29.4: At-rest lateral earth pressure using the ASCE 4-98 method



RAI Figure 02.05.04-29.5: ARS at ground surface for Unit 2 structural fill (Annex Building)



RAI Figure 02.05.04-29.6: Peak ground acceleration for Unit 2 structural fill (Annex Building)



RAI Figure 02.05.04-29.7: Comparison of Site-Specific At-rest Lateral Earth Pressure (ASCE 4-98 Method) and Westinghouse AP 1000 Design Pressures

NRC RAI Letter No. 032 Dated February 12, 2009

SRP Section: 2.5.4 – Stability of Subsurface Materials and Foundations

Question from Geosciences and Geotechnical Engineering Branch 1 (RGS1)

NRC RAI Number: 02.05.04-30

FSAR Section 2.5.4.10.3 indicates that lateral pressure effects due to potential soil compaction are not included in the lateral pressure computation. References such as “Compaction-Induced Earth Pressures Under K_0 -Conditions” by Duncan and Seed indicate that significant lateral pressures may be developed even with use of light compaction equipment. Please provide information on the planned compaction procedures to be used, impact on lateral pressures, reduced compacted density and shear wave velocity which may impact horizontal SSI response.

VCSNS RESPONSE:

References 1 and 2 contain a procedure to evaluate the compaction-induced lateral earth pressures for at-rest conditions, such as lateral earth pressures against the below-grade walls of the nuclear island that are not allowed to rotate away from the backfill (non-yielding walls). References 1 and 2 provide the dimensions and loads of various compactors including heavy vibratory compactors, walk-behind vibratory rollers, and vibratory plate compactors, and the relevant design charts for compaction-induced lateral earth pressure under various line loads. Reference 2 provides an updated version of adjustment factors for the compaction-induced lateral earth pressures caused by heavy compactors. These factors are based on lift thickness, distance from the wall to the edge of the compactor, roller width, and the friction angle of the soil being compacted. Based on other studies, Reference 2 states that it is possible to compact backfill to the same density using two different compactors, one of which induces much higher lateral pressures than the other one; and vibratory compactors are more effective than static or rammer compactors in densifying cohesionless soils without inducing high lateral pressures. For the most part, the use of heavy compaction equipment close to below-grade walls (within 5 ft) is discouraged. FSAR Subsection 2.5.4.5.3.1 states that compaction is performed with a heavy steel-drummed vibratory roller, except within 5 ft of a structure wall, where smaller compaction equipment is used to minimize excess pressures against the wall. Fill placement and compaction control procedures will be addressed in a technical specification. Nevertheless, the influence of compaction on the lateral earth pressure is evaluated below.

As part of this evaluation, the methodology described in References 1 and 2 is pursued to compute the compaction-induced pressures under at-rest conditions. The pressure diagram associated with the assumed compactor is derived from RAI Figure 02.05.04-30.1 (from Reference 2, Figure 14). This pressure diagram applies to static or vibratory

rollers (other available design charts are for vibratory plates and rammers). On this figure, curves are developed for line loads (q) of 200, 400, 600, and 800 lb/in. At-rest earth pressure curves are superimposed on the curves for various q values. To be on the conservative side, the highest available line load ($q = 800$ lb/in) is selected, which produces the highest lateral pressure. For conditions other than those on which the charts are based, adjustments are made using the multiplier factors in RAI Table 02.05.04-30.1 (from Reference 2, Table 12).

The conditions selected in this evaluation are: roller width = 7 ft, distance from the wall to the edge of the compactor = 0.5 ft, and lift thickness = 0.5 ft. For these selected values all multiplier factors are equal to 1.0. Only the friction angle multiplier for the backfill type selected (i.e., $\phi' = 36^\circ$) needs to be adjusted. For this backfill type, unit weight $\gamma = 125$ pcf and at-rest pressure coefficient $K_0 = 0.5$. Thus the at-rest pressure is equal to 62.5 psf ($125 \text{ pcf} \times 0.5$) times depth. By equating the at-rest pressure to the compaction-induced pressure, these pressures are found to coincide at a depth of about 16.5 ft (which is above the groundwater level), at a lateral pressure of about 1,025 psf. Below this depth, at-rest pressures exceed compaction-induced pressures. RAI Figure 02.05.04-30.2 illustrates the compaction-induced lateral earth pressures caused by heavy compactors for at-rest earth pressure conditions. Refer to the response to RAI 2.5.4-29 for detailed information on the development of other components of the at-rest earth pressure diagram.

Note that from RAI Table 02.05.04-30.1, for distances from the wall to the edge of compactor of 0.0 ft and 0.5 ft, the multiplier factor is 1.0; therefore the same pressure distribution shown in RAI Figure 02.05.04-30.2 applies to distances from the wall ranging from 0.0 to 0.5 ft. At a distance of 1 ft from the wall, from the same table, the compaction-induced pressures are reduced by 10 to 13% depending on the depths from ground surface (i.e., 2, 4, 8 and 16 ft). The adjustment factors are not available for distances beyond 1.0 ft. However, it can be concluded that this procedure will result in low compaction-induced lateral earth pressures for cases where the edge of the compactor is located 5 ft or more away from the back of the below-grade wall.

Reference 3 (DM 7.2, p. 7.2-76) contains a procedure to evaluate the compaction-induced lateral earth pressures for active conditions, i.e., lateral earth pressures against walls that are allowed to rotate away from the backfill. However, in the proposed nuclear island area, no permanent retaining wall type structures are planned; therefore, the compaction-induced lateral earth pressures for active conditions are not presented here.

References

1. Duncan, J.M., G.W. Williams, A.L. Sehn and R.B. Seed (1991). "Estimation of Earth Pressures due to Compaction", *Journal of Geotechnical Engineering*, ASCE, New York, NY, 117(12):1833-1847.

2. Duncan, J.M., G.W. Williams, A.L. Sehn and R.B. Seed (1993). "Closure of 'Estimation of Earth Pressures due to Compaction'", *Journal of Geotechnical Engineering*, ASCE, New York, NY, 119(7):1172-1177.
3. NAVFAC (Revalidated-1986). Naval Facilities Engineering Command. "Foundations & Earth Structures", *Design Manual 7.02*, Alexandria, VA.

This response is PLANT SPECIFIC.

ASSOCIATED VCSNS COLA REVISIONS:

The following FSAR changes will be incorporated in a future revision of the COLA.

1. The first sentence of the first paragraph of FSAR Subsection 2.5.4.10.3 will be revised as follows:

Static and seismic lateral earth pressures are addressed for plant underground walls with a height of 45 40 feet (e.g., to about 5 feet below the base of the nuclear island for the typical underground wall height of the nuclear island in the AP1000 design).

2. The last sentence of the first paragraph of FSAR Subsection 2.5.4.10.3 will be revised as follows:

Lateral pressures due to compaction are not included; these pressures are controlled by compacting backfill with light equipment near structures. conservatively included in the pressure diagrams. Note that FSAR Subsection 2.5.4.5.3.1 states that compaction is performed with a heavy steel-drummed vibratory roller, except within 5 ft of a structure wall, where smaller compaction equipment is used to minimize excess pressures against the wall. Fill placement and compaction control procedures are addressed in a technical specification.

3. The last sentence of the second paragraph of FSAR Subsection 2.5.4.10.3 will be revised as follows:

The peak horizontal ground acceleration of 0.55g was used for developing the seismic active earth pressure diagrams (i.e., $k_h=0.55$) (obtained for in-situ soils) is conservatively used for developing the seismic active earth pressure diagrams (i.e., $k_h=0.55$), even though the peak horizontal ground acceleration obtained for the structural fill is 0.38g. As recommended in Reference 257 (ASCE 4-98, Section 3.5.3.3), the Mononobe-Okabe method (Reference 242) is used to establish seismic lateral active earth pressures, provided that wall displacements required to develop the active earth pressure are tolerated without loss of wall function.

4. The last two sentences of the third paragraph of FSAR Subsection 2.5.4.10.3 will be eliminated and a new paragraph begun, as follows:

~~This method was used to estimate the seismic lateral at-rest pressures against the buried structure walls. The response spectrum at the bottom of the nuclear island was used in this analysis.~~

Another approach to estimating the seismic lateral earth pressure against buried, non-yielding walls is the elastic solution recommended in ASCE 4-98 (Reference 257). This solution contains a nomograph in which a dimensionless normal stress diagram at 1.0g horizontal earthquake acceleration is displayed for a normalized depth at a given Poisson's Ratio. Following the recommendation in ASCE 4-98, this elastic solution is used to estimate the seismic lateral at-rest pressures against buried structure walls. The peak horizontal ground acceleration of 0.38g (obtained for the structural fill) is used for developing the seismic at-rest earth pressure diagram. This is the seismic lateral earth pressure shown in Figure 2.5.4-244.

For the compaction-induced pressures under at-rest conditions, the methodology described in References 254 and 255 is used. To be on the conservative side, the highest available line load ($q = 800$ lb/in) is selected, which produces the highest lateral pressure. This is the compaction induced pressure under at-rest conditions shown in Figure 2.5.4-244. As noted earlier, this is conservative since FSAR Subsection 2.5.4.5.3.1 states that compaction is performed with a heavy steel-drummed vibratory roller, except within 5 ft of a structure wall, where smaller compaction equipment is used to minimize excess pressures against the wall.

Reference 256 contains a procedure to evaluate the compaction-induced lateral earth pressures for active conditions, i.e., lateral earth pressures against walls that are allowed to rotate away from the backfill. However, in the proposed nuclear island area, no permanent retaining wall type structures are planned; therefore, the compaction-induced lateral earth pressures for active conditions are not presented here.

5. Update Figure 2.5.4-243 (active) with **RAI Figure 02.05.04-29.2** from the response to RAI 02.05.04-29.
6. Update Figure 2.5.4-244 (at-rest) with **RAI Figure 02.05.04-30.2**.
7. Add the following references to FSAR Section 2.5.4:

254. Duncan, J.M., G.W. Williams, A.L. Sehn and R.B. Seed. "Estimation of Earth Pressures due to Compaction", *Journal of Geotechnical Engineering*, ASCE, New York, NY, 117(12):1833-1847, 1991.

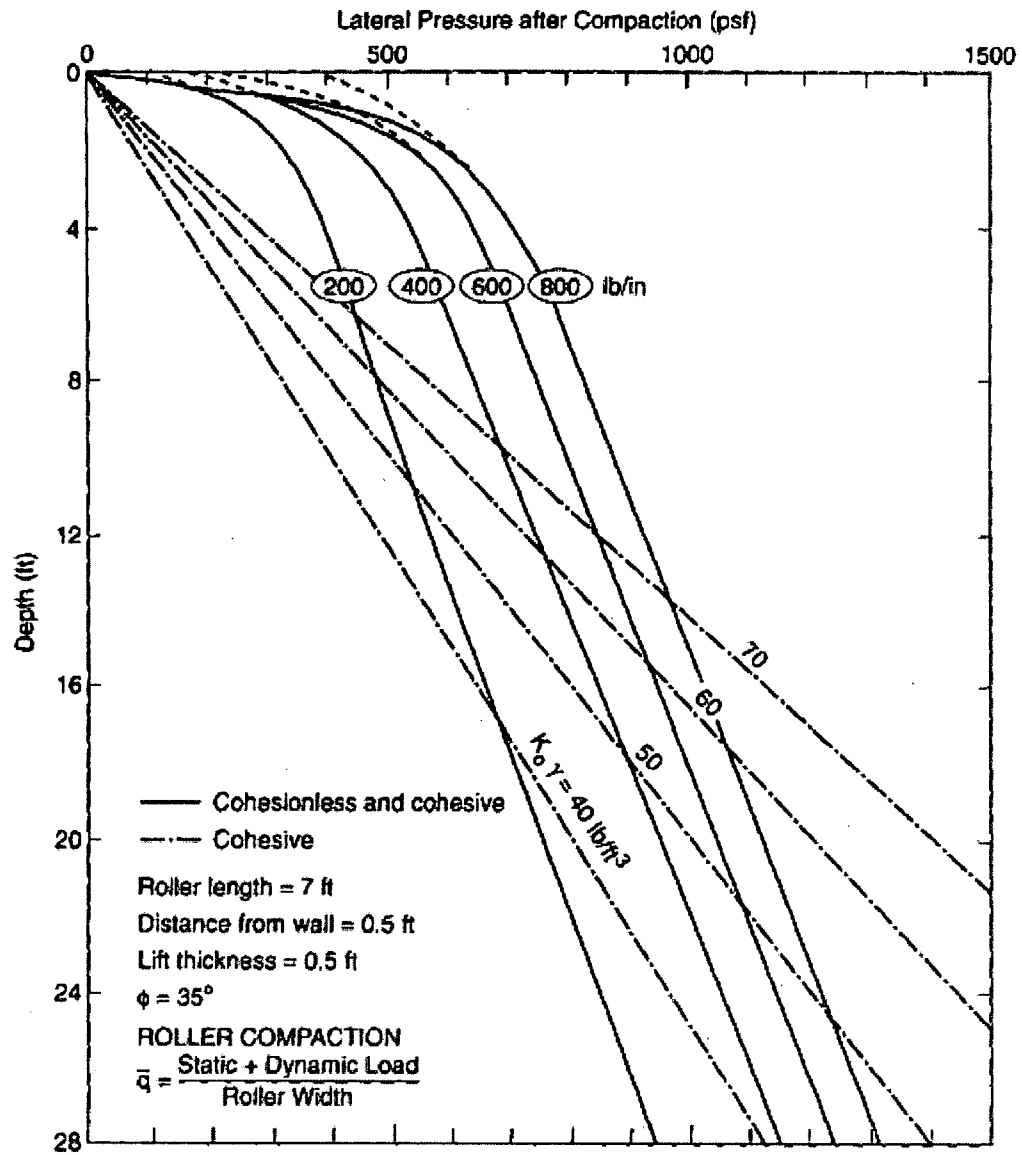
255. Duncan, J.M., G.W. Williams, A.L. Sehn and R.B. Seed. "Closure of 'Estimation of Earth Pressures due to Compaction'", *Journal of Geotechnical Engineering*, ASCE, New York, NY, 119(7):1172-1177, 1993.
256. Department of Navy. *Foundations and Earth Structures, Design Manual 7.2*, Alexandria, VA. pp 7.2-76-77, 1982.
257. ASCE 4-98. *Seismic Analysis of Safety-Related Nuclear Structures and Commentary*. ASCE, Reston, VA, 2000.

ASSOCIATED ATTACHMENTS:

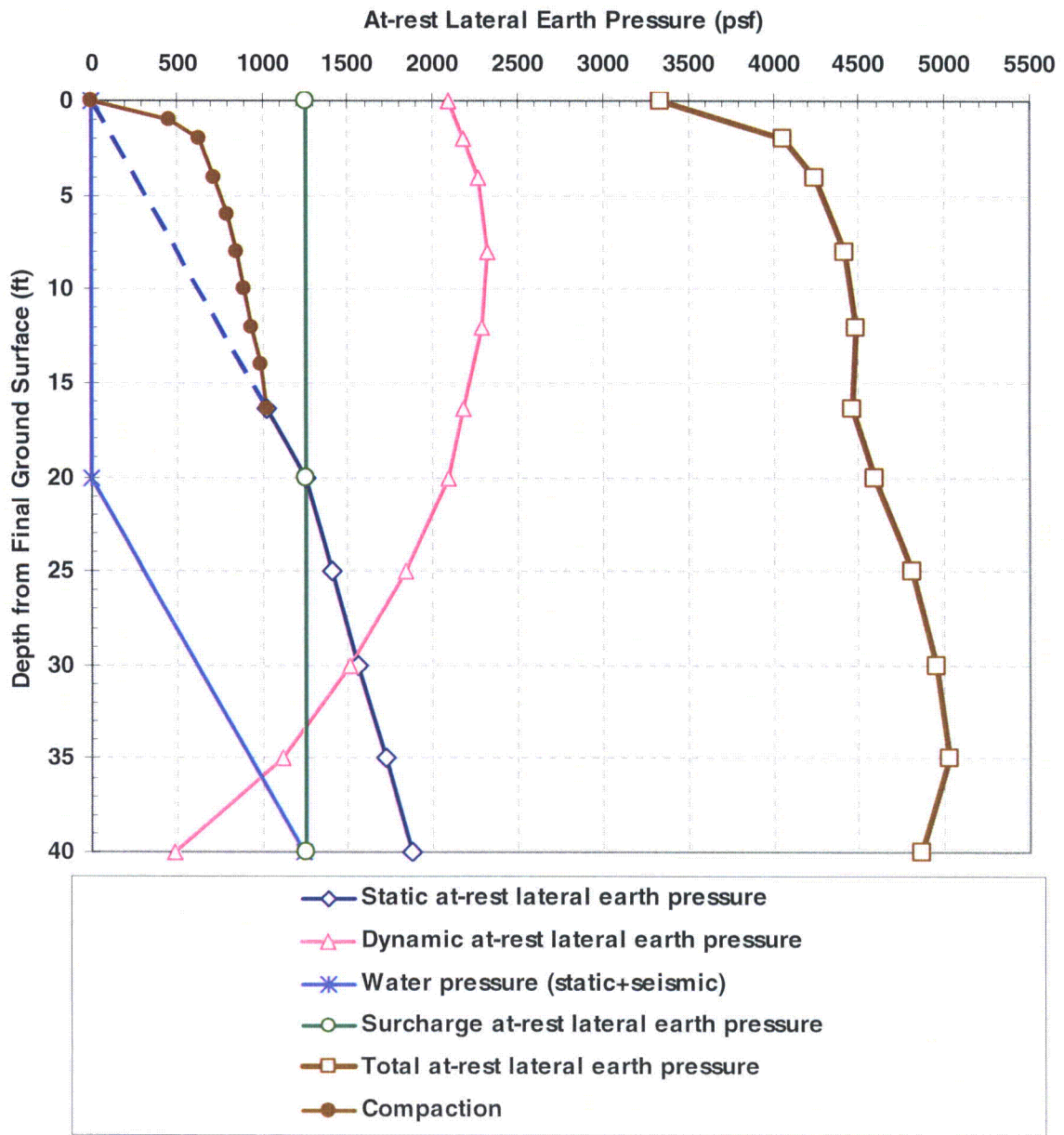
RAI Table 02.05.04-30.1;
RAI Figures 02.05.04-30.1 and 02.05.04-30.2

RAI Table 02.05.04-30.1 Adjustment Factors for Earth Pressures due to Compaction by Rollers (Reference 2, Table 12)

Variables (1)	Multiplier Factors for $z =$			
	2 ft (2)	4 ft (3)	8 ft (4)	16 ft (5)
(a) Lift Thickness (t) and Distance from Wall (x) (Adjustment Factors are Combined)				
$x = 0.00 \text{ ft}^a$	1.00	1.00	1.00	1.00
$x = 0.20 \text{ ft}^a$	1.00	1.00	1.00	1.00
$x = 0.50 \text{ ft}^a$	1.00	1.00	1.00	1.00
$x = 1.00 \text{ ft}^a$	0.87	0.88	0.89	0.90
$x = 0.00 \text{ ft}^b$	0.94	0.95	0.95	0.96
$x = 0.20 \text{ ft}^b$	0.94	0.95	0.95	0.96
$x = 0.50 \text{ ft}^b$	0.94	0.95	0.95	0.96
$x = 1.00 \text{ ft}^b$	0.83	0.84	0.86	0.88
(b) Roller Width (w)				
$w = 1.25 \text{ ft}$	0.80	0.80	0.80	0.88
$w = 3.50 \text{ ft}$	0.96	0.94	0.94	0.97
$w = 7.00 \text{ ft}$	1.00	1.00	1.00	1.00
$w = 10.00 \text{ ft}$	1.00	1.01	1.02	1.04
(c) Friction Angle (ϕ)				
$\phi = 25^\circ$	0.59	0.70	0.81	0.96
$\phi = 30^\circ$	0.75	0.83	0.89	0.98
$\phi = 35^\circ$	1.00	1.00	1.00	1.00
$\phi = 40^\circ$	1.23	1.16	1.10	1.03
$^a t = 0.5 \text{ ft.}$				
$^b t = 1.0 \text{ ft.}$				
Note: 1 ft = 0.3048 m.				



RAI Figure 02.05.04-30.1 Earth Pressure due to Compaction by Rollers (Reference 2, Figure 14)



RAI Figure 02.05.04-30.2 (updated FSAR Figure 2.5.4-244 – same as RAI Figure 02.05.04-29.4)